Acta Oceanol. Sin., 2023, Vol. 42, No. 4, P. 25–32
https://doi.org/10.1007/s13131-022-2087-0
http://www.aosocean.com
E-mail: ocean2@hyxb.org.cn

Potential effects of sea level rise on the soil-atmosphere greenhouse gas emissions in *Kandelia obovata* mangrove forests

Jiahui Chen[1], Shichen Zeng[1], Min Gao[1], Guangcheng Chen[2, 3], Heng Zhu[1], Yong Ye[1]*

[1] Key Laboratory of the Ministry of Education for Coastal and Wetland Ecosystems, College of the Environment and Ecology, Xiamen University, Xiamen 361102, China

[2] Third Institute of Oceanography, Ministry of Natural Resources, Xiamen 361005, China

[3] Fujian Provincial Station for Field Observation and Research of Island and Coastal Zone in Zhangzhou, Xiamen 361005, China

Received 21 February 2022; accepted 27 June 2022

Abstract

Mangrove forests are under the stress of sea level rise (SLR) which would affect mangrove soil biogeochemistry. Mangrove soils are important sources of soil-atmosphere greenhouse gas (GHG) emissions, including carbon dioxide (CO_2), methane (CH_4) and nitrous oxide (N_2O). Understanding how SLR influences GHG emissions is critical for evaluating mangrove blue carbon capability. In this study, potential effects of SLR on the GHG emissions were quantified through static closed chamber technique among three sites under different intertidal elevations, representing tidal flooding situation of SLR values of 0 cm, 40 cm and 80 cm, respectively. Compared with Site SLR 0 cm, annual CO_2 and N_2O fluxes decreased by approximately 75.0% and 27.3% due to higher soil water content, lower salinity and soil nutrient environments at Site SLR 80 cm. However, CH_4 fluxes increased by approximately 13.7% at Site SLR 40 cm and 8.8% at Site SLR 80 cm because of lower salinity, higher soil water content and soil pH. CO_2-equivalent fluxes were 396.61 g/(m^2·a), 1 423.29 g/(m^2·a) and 1 420.21 g/(m^2·a) at Sites SLR 80 cm, SLR 40 cm and SLR 0 cm, respectively. From Site SLR 0 cm to Site SLR 80 cm, contribution rate of N_2O and CH_4 increased by approximately 7.42% and 3.02%, while contribution rate of CO_2 decreased by approximately 10.44%. The results indicated that warming potential of trace CH_4 and N_2O was non-negligible with SLR. Potential effects of SLR on the mangrove blue carbon capability should warrant attention due to changes of all three greenhouse gas fluxes with SLR.

Key words: carbon dioxide, methane, nitrous oxide, CO_2-equivalent fluxes, sea level rise, mangrove forest

Citation: Chen Jiahui, Zeng Shichen, Gao Min, Chen Guangcheng, Zhu Heng, Ye Yong. 2023. Potential effects of sea level rise on the soil-atmosphere greenhouse gas emissions in *Kandelia obovata* mangrove forests. Acta Oceanologica Sinica, 42(4): 25–32, doi: 10.1007/s13131-022-2087-0

1 Introduction

The accelerating rate of sea level rise (SLR) is causing coastal ecosystem changes on a global scale (Meeder et al., 2021). The global mean sea level is projected to rise between 0.28 m and 0.98 m by the end of the 21st century based on the sea level of 2000 according to the Representative Concentration Pathway Scenarios, hence posing a major challenge for coastal regions worldwide (IPCC, 2013; Jayanthi et al., 2018; Perera et al., 2018; Mafi-Gholami et al., 2020). Mangrove forests as the only forests between land and sea are vulnerable to SLR (Krauss et al., 2014; Lovelock et al., 2015; Chen and Wang, 2017; Langston et al., 2017; Minick et al., 2019; Kirwan and Gedan, 2019). If soil accumulation rate is less than the rate of sea level rise, SLR will change water movement, alter tidal variation, and increase seawater intrusion into mangrove forests, resulting in both deeper flooding level, longer flooding duration and more anaerobic conditions (Ye et al., 2010; Wang et al., 2019). Therefore, SLR potentially has a substantial effect on the mangrove ecosystem.

The global wetland area accounts for 10% of the earth's surface area, but stores 15% of earth's total terrestrial carbon (Davidson et al., 2018; Sheng et al., 2021; Zhang et al., 2021). Although mangrove forests occupy a limited area compared with terrestrial forests, mangrove forests are increasingly seen as highly productive and most carbon-rich ecosystems among all coastal wetlands (Donato et al., 2011; McLeod et al., 2011). The average global carbon stock in the mangrove soils is approximately 720 t/hm^2 (Alongi, 2014). Carbon stored in the mangrove ecosystems, along with salt marshes and seagrass beds, is termed "blue carbon" and has become a topic of global interest (Capooci et al., 2019). Meanwhile, mangrove ecosystems are known to constitute a net source of greenhouse gases including carbon dioxide (CO_2), methane (CH_4) and nitrous oxide (N_2O) (Chen et al., 2010, 2012, 2015, 2016). Emissions of these three greenhouse gases exchanged between mangrove soils and the atmosphere, reduce soil carbon stock and the contribution of mangrove plants to the atmospheric cooling effect (Chen et al., 2015, 2016). For CO_2, this emission rates from mangrove soil tended to be higher when soils were exposed to the atmosphere than when they were im-

Foundation item: The National Natural Science Foundation of China under contract Nos 42076142 and 41776097; the Provincial Natural Science Foundation of Fujian under contract No. 2020J06030; the Fund of Fujian Provincial Key Laboratory of Marine Ecological Conservation and Restoration under contract No. EPR2020003.
*Corresponding author, E-mail: yeyong@xmu.edu.cn

mersed by tides, due to the faster molecular diffusion for gases than fluids, as well as the increased surface area for aerobic respiration and chemical oxidation (Chen et al., 2012). For CH_4, the increase in the SO_4^{2-} carried by tidal flooding due to SLR could suppress CH_4 production (Stumm and Morgan, 1981). In addition, N_2O production is favored due to the alternation between dry and wet conditions and is more likely to occur during low levels of O_2 (Liikanen and Martikainen, 2003; Jørgensen and Elberling, 2012; Capooci et al., 2019). Changes of mangrove soil conditions due to SLR will affect mangrove greenhouse gas emissions, further influencing mangrove blue carbon capability. Although previous studies (Rogers et al., 2019; Chen et al., 2020b) have found that SLR will increase the stocks of organic carbon (OC) in mangrove soils, the direct field observations for responses of greenhouse gas emissions from mangrove ecosystems to SLR remain unexplored.

Therefore, in the present study, potential effects of SLR on the soil-atmosphere greenhouse gas emissions (CO_2, CH_4 and N_2O) were quantified among three sites under different intertidal elevations in 9 years-old *Kandelia obovata* mangrove forests, representing tidal flooding situations of different SLR values. We posed the following research questions: (1) How higher sea levels could affect mangrove soil-atmosphere greenhouse gas emissions? (2) What are possible mechanisms of changes in mangrove soil-atmosphere greenhouse gas emissions with SLR?

2 Materials and methods

2.1 *Study area and plot arrangements*

The study area is located along the coastline of Zengying (24°33′9.24″N, 118°02′3.71″E) in Xiamen, Fujian, China (Fig. 1). This region is characterized by a subtropical marine monsoonal climate, with annual mean rainfall of 1 097 mm and the rainy season from April to June. Mean annual air temperature is 20.8℃ and average annual insolation duration is 2 276 h (Chen and Ye, 2013). March to May, June to August, September to November and December to February are categorized as spring, summer, autumn and winter months, respectively. Tides are semi-diurnal, with an average range of 4 m. Salinity of seawater adjacent to mangrove area ranges from 26 to 30 (Chen and Ye, 2013, 2014). Altitude of local mean sea level in Xiamen Bay is 365 cm (Ruan et al., 2010).

Many aquaculture ponds with boulder strips were used to breed crabs in this intertidal zone before 2002. These ponds were deserted and cofferdams around them were demolished after 2002. Soil with similar soil physico-chemical properties beside these ponds were used to transform three adjacent ponds for mangrove planting sites (Chen and Ye, 2013, 2014; Chen et al., 2020b). The final steady differences in elevation between two nearby sites were 40 cm, with sea level altitudes of 335 cm, 375 cm and 415 cm for the lower (SLR 80 cm), middle (SLR 40 cm) and upper (SLR 0 cm) elevation, respectively. According to the Ocean Blue Book on Climate Change in China (Liu et al., 2019), the average increase in sea level in China was 3.3 mm/a (33 cm per 100 a, 66 cm per 200 a) from 1980 to 2018. Elevation differences among the three sites were used to represent different tidal flooding situations that might be expected with rising sea level. Sea levels at Sites SLR 0 cm, SLR 40 cm and SLR 80 cm represented tidal flooding time of the current (Site SLR 0 cm), future ~100 a's (Site SLR 40 cm) and future ~200 a's SLR (Site SLR 80 cm) of mangrove forests along the Jiulong River Estuary, approximately 22 km away from the study area. Sites SLR 80 cm, SLR 40 cm and SLR 0 cm had mean inundation time of 10 h/d, 8 h/d and 6 h/d (i.e., 5 h, 4 h and 3 h per tide), respectively, measured during one whole tide cycle of 15 d in August 2004 (Chen and Ye, 2014). According to our previous study (Chen et al., 2020b), before mangrove planting, the soils among the three sites have similar soil physico-chemical properties including pH (p=0.452, one-way ANOVA), water content (p=0.566, one-way ANOVA), soil salinity (p=0.628, one-way ANOVA) and soil OC content (p=0.977, one-way ANOVA). In May 2004, the healthy mature *K. obovata* propagules were planted at the three sites and *K. obovata* among the three sites became the dominant species with 9 years-old at the sampling time of the present study. In the field observation, pol-

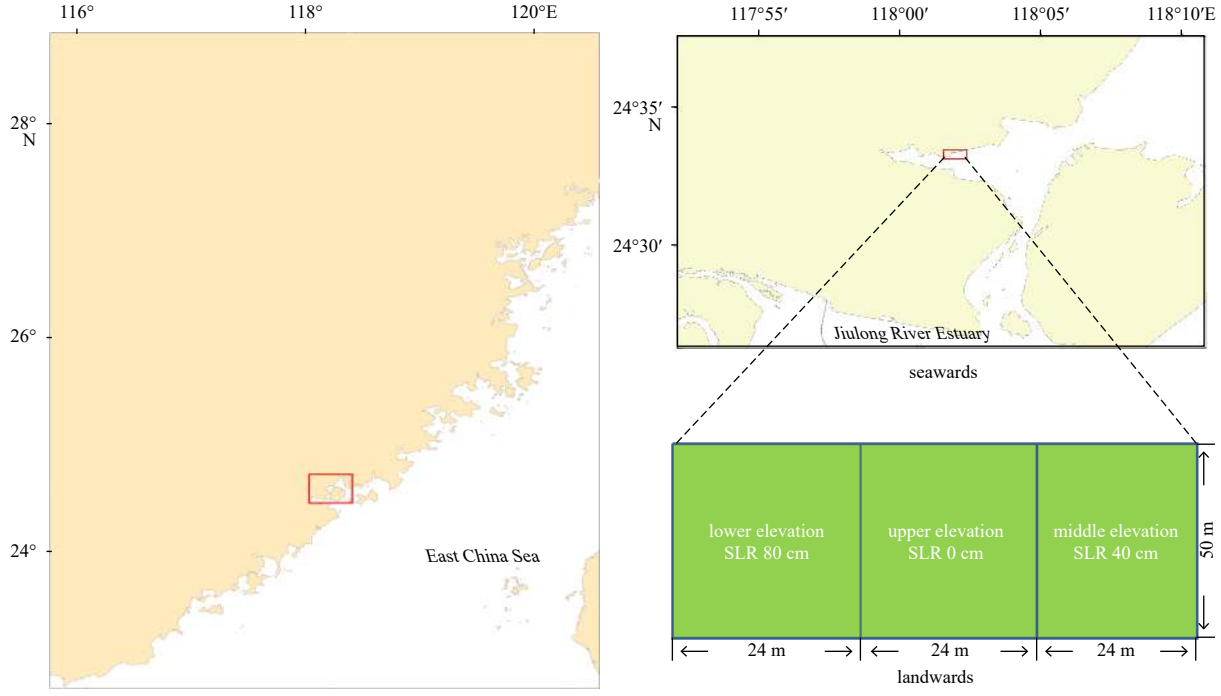

Fig. 1. Maps of Zengying, the study area. SLR: sea level rise.

lutants (e.g., wastewater from aquaculture) which affected mangrove soil-atmosphere greenhouse gas emissions were not found to enter into the three sites from land and sea.

2.2 *Gas sampling and flux measurement*

Methods of collecting soil-atmosphere greenhouse gas fluxes have been reported in the previous studies (Chen et al., 2010, 2015, 2016). In brief, soil-atmosphere greenhouse gas fluxes were sampled monthly throughout the whole year from June 2013 to May 2014 at the three sites. Three replicates (each was approximately 10 m apart) for each site were applied in gas sampling using static closed chamber technique, and all samplings were conducted two hours before the lowest tide during the daytime. The static transparent chambers with a diameter of 17 cm (total area coverage of 0.023 m^2) and a headspace volume over the soil of 1.47 L were applied in sampling. Each chamber was lightly inserted 2.5 cm into the soil at locations with no aboveground vegetation or litter fall. At 0 min, 15 min and 30 min after closure, a 5 mL gas sample was collected by passing a 10 mL glass syringe through the sampling outlet and was then immediately injected into dark airtight containers which were made of rubber stopper and aluminum foil.

During sample analysis, 1 mL gas sample was analyzed within 12 h using a gas chromatography system (Agilent 7890A, Santa, Clara, CA, USA) to determine concentrations of N_2O, CH_4 and CO_2 and the standard was analyzed in every 6 samples (Chen et al., 2010, 2015, 2016). N_2O concentration was determined with a ^{63}Ni electron capture detector (μECD). CH_4 and CO_2 concentrations were analyzed with a flame ionization detector (FID). Gas concentrations were determined by comparing the sample peak areas against the standard curves (Agilent Greenhouse Gas Checkout Sample). Each soil-atmosphere greenhouse gas flux was calculated using the difference between the two points in the time series of concentration for each plot.

The soil-atmosphere flux (F, mol/(m^2·h)) of each greenhouse gas was calculated by following formula:

$$F = (V \times \Delta M)/(A \times P), \tag{1}$$

where F was the interfacial gas flux (mol/(m^2·h)), V was the internal air volume (m^3) in the container after the pot was placed, ΔM (h^{-1}) was the change in gas concentration in the container, A was the surface area of the soil (m^2) and P was the volume of per molar gas (m^3/ mol).

2.3 *Soil sampling and analysis*

Soil samples (5 cm depth) were immediately collected for measurement of soil properties including organic carbon (OC), total nitrogen (TN) and total phosphorus (TP) after gas sampling was completed. Rapid dichromate oxidation procedure was used to determine soil OC content and a continuous flow analyzer (Futura II, Alliance Instruments, France) was used to determine soil TN and TP after Kjeldahl digestion (Allen et al., 1974). All data were expressed as the 105℃ dry weight. Moreover, air temperature which was used to calculate soil-atmosphere greenhouse gas fluxes was measured by atmosphere thermometer (digital thermometer, TP101) during sampling period.

2.4 *Estimates of annual greenhouse gas emission and CO_2-equivalent fluxes*

Each annual greenhouse gas flux was further estimated based on the summation for monthly measurement during the entire year from June 2013 to May 2014. Annual gas fluxes were then converted to CO_2-equivalent fluxes (F_e, g/(m^2·a)) by the following equation according to Myhre et al. (2013):

$$F_e = R_{N_2O} \times 298 + R_{CH_4} \times 34 + R_{CO_2} \times 1, \tag{2}$$

where R_{N_2O}, R_{CH_4} and R_{CO_2} denote annual emission rates of N_2O (g/(m^2·a)), CH_4 (g/(m^2·a)) and CO_2 (g/(m^2·a)), respectively.

2.5 *Statistical analyses*

Normality of each variable was examined using Kolmogorov–Smirnov test, and homoscedasticity was examined with Kaiser-Meyer-Olkin index and Bartlett's test of sphericity. Main and interactive effects of SLR and sampling months on each greenhouse gas flux and soil properties were analyzed using two-way analysis of variance (ANOVA), with pairwise comparisons of interactive effects conducted using post hoc Tukey's HSD test. Pearson correlation was used to describe relationships between greenhouse gas fluxes and soil properties. All statistical analyses were performed using SPSS 22.0 for Windows (SPSS, Chicago, IL, USA).

3 Results

3.1 *Greenhouse gas fluxes*

Both SLR (F=9.522, P<0.001) and months (F=4.479, P<0.001) had significant impacts on the N_2O fluxes (Table 1). This parameter showed a decreasing order of Site SLR 0 cm ((0.57±0.28) μmol/(m^2·h)), Site SLR 80 cm ((0.41±0.26) μmol/(m^2·h)), Site SLR 40 cm ((0.28±0.14) μmol/(m^2·h)). Significantly higher N_2O fluxes were determined either in spring or summer months than that in autumn or winter months (Fig. 2). The lowest values were obtained in October at Sites SLR 40 cm and SLR 0 cm while in November at Site SLR 80 cm.

In contrast to N_2O fluxes, significant differences of CH_4 fluxes were only found among different months (F=9.563, P<0.001) (Table 1). The lowest values were found in December at Sites SLR 80 cm and SLR 0 cm while in October at Site SLR 40 cm, and this parameter peaked in August at Sites SLR 0 cm and SLR 40 cm, and September at Site SLR 80 cm (Fig. 2). Contrary to the trend in the N_2O fluxes, annual CH_4 fluxes were highest at Site SLR 40 cm ((3.56±2.57) μmol/(m^2·h)), followed by Site SLR 80 cm ((3.41±2.88) μmol/(m^2·h)) and Site SLR 0 cm ((3.13±2.81) μmol/(m^2·h)).

Annual CO_2 fluxes were (0.87±3.48) mmol/(m^2·h), (3.56±

Table 1. The interfacial gas flux (F) values of two-way ANOVA tests showing the effects of sea level rise (SLR) and month on the soil-atmosphere greenhouse gas fluxes and soil properties

Sources of variation	df	Parameter						
		OC	TN	TP	C/N	N_2O flux	CH_4 flux	CO_2 flux
SLR	2	257.387***	168.866***	74.294***	31.207***	9.522***	0.273	62.963***
Month	11	14.318***	22.277***	17.372***	2.588**	4.479***	9.563***	56.088***
Interaction	22	7.284***	12.441***	3.778***	3.312***	1.357	2.195*	6.589***

Note: *, ** and *** indicate significant difference at p<0.05, p<0.01 and p<0.001, respectively. OC: organic carbon; TN: total nitrogen; TP: total phosphorus; C/N: C/N content ratio; SLR: sea level rise.

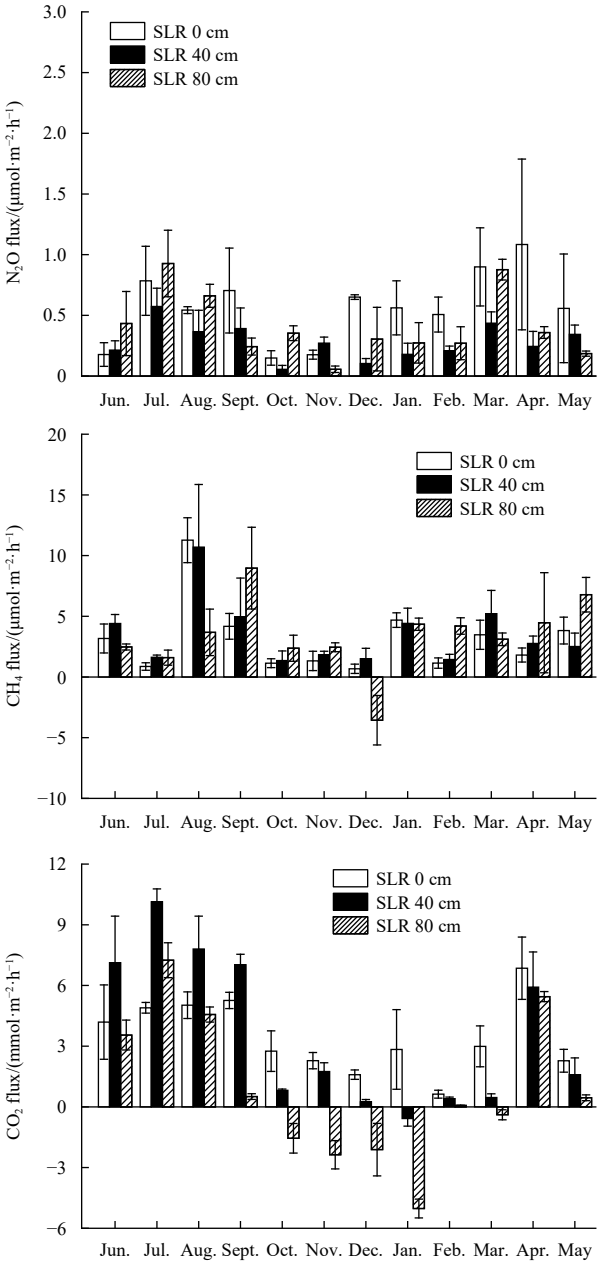

Fig. 2. Temporal variation of N_2O, CH_4 and CO_2 fluxes from soils at the three *Kandelia obovata* forests (mean±SE, SLR: sea level rise).

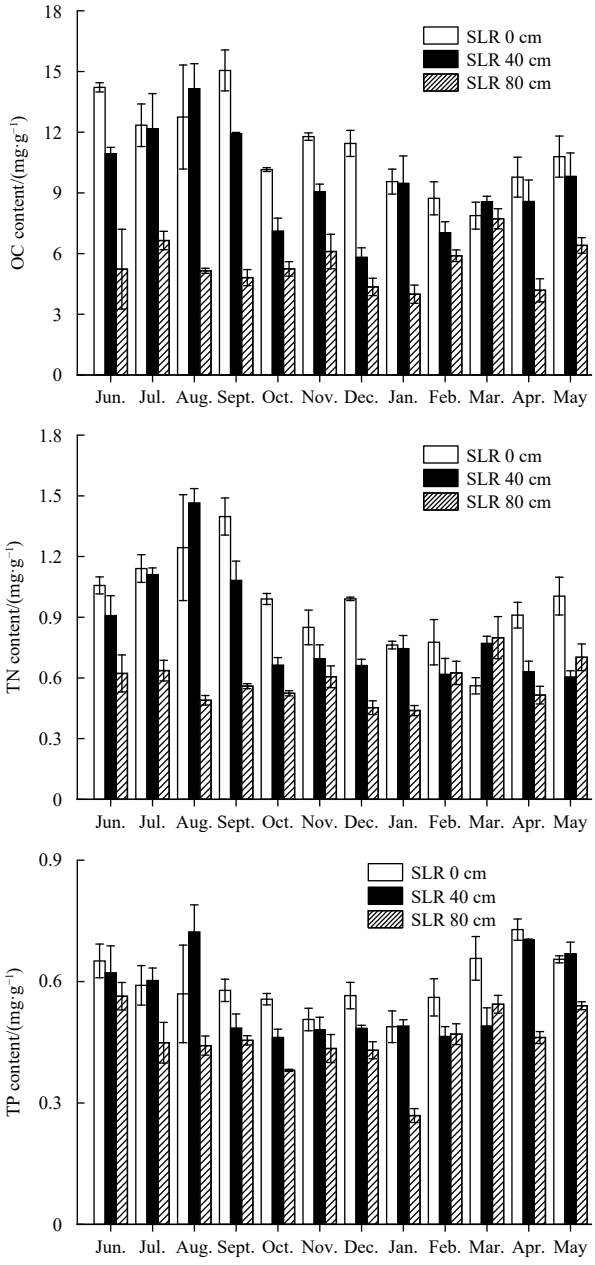

Fig. 3. Temporal variation in surface (0–5 cm) soil organic carbon (OC), total nitrogen (TN), total phosphorus (TP) and C/N content ratio at the three *Kandelia obovata* forests (mean±SE, SLR: sea level rise).

3.58) mmol/(m²·h) and (3.47±1.71) mmol/(m²·h) at Sites SLR 80 cm, SLR 40 cm and SLR 0 cm, respectively. SLR (F=62.963, P<0.001), month (F=56.088, P<0.001) and their interaction (F=6.589, P<0.001) had significant effects on the CO_2 fluxes (Table 1, Fig. 2). This parameter showed an obvious temporal variation at all three sites, with lower values in autumn or winter months than that in spring or summer months. Although mangrove soils at Sites SLR 40 cm and SLR 80 cm were sources of CO_2 over the entire year, they occasionally showed consumption of atmospheric CO_2 especially during the cold months.

3.2 *Soil properties*

SLR (F=257.387, P<0.001) and month (F=14.318, P<0.001) had a significant interaction in terms of soil OC content at the three sites, which gradually decreased with SLR (Table 1, Fig. 3). Soil OC contents were (5.48±1.07) mg/g, (9.55±2.31) mg/g and (11.21±2.06) mg/g at Sites SLR 80 cm, SLR 40 cm and SLR 0 cm, respectively. At the three sites, a significant temporal trend of soil OC content was detected, with the highest value occurring either in spring or summer months.

Soil TN contents were (0.58±0.10) mg/g, (0.83±0.25) mg/g and (0.97±0.22) mg/g at Sites SLR 80 cm, SLR 40 cm and SLR 0 cm, respectively. SLR (F=168.866, P<0.001) and month (F=22.277, P<0.001) had a significant interaction (F=12.441, P<0.001) on the soil TN contents, which decreased with SLR (Table 1, Fig. 3). Significantly higher soil TN contents were determined in summer at Site SLR 40 cm, in autumn at Site SLR 0 cm while in spring at Site SLR 80 cm. Differences were observed throughout the whole year, with the values exhibiting the following order: SLR 80 cm < SLR

40 cm < SLR 0 cm. C/N content ratios were also significantly affected by SLR (F=31.207, P<0.001) and month (F=2.588, P<0.01) (Table 1), and the values were comparable between Sites SLR 40 cm and SLR 0 cm, with lower values observed at Site SLR 80 cm (Fig. 3).

Soil TP contents were at a less variable level throughout the entire year with mean values of (0.45±0.08) mg/g, (0.56±0.10) mg/g and (0.59±0.07) mg/g at Sites SLR 80 cm, SLR 40 cm and SLR 0 cm, respectively. SLR (F=74.294, P<0.001) and month (F=17.372, P<0.001) had a significant interaction (F=3.778, P<0.001) on this parameter which decreased with SLR (Table 1, Fig. 3). Significant temporal trends of soil TP content were detected with the highest value occurring either in spring or summer months at the three sites.

3.3 *Relationships between greenhouse gas and soil parameters*

As shown in Table 2, there was a significantly positive correlation between N_2O flux and soil TP content. CH_4 flux was significantly positively correlated with soil TN content, but not with soil TP content. In comparison to N_2O and CH_4 fluxes, CO_2 fluxes were strongly positively correlated with soil OC, TN and TP contents.

3.4 *Annual emission of greenhouse gases and CO_2-equivalent fluxes*

Annual N_2O emissions at Sites SLR 80 cm and SLR 40 cm were 159.83 mg/(m²·a) and 108.98 mg/(m²·a), which were lower than that at Site SLR 0 cm (218.65 mg/(m²·a)). On the contrary, compared with annual CH_4 emissions at Site SLR 0 cm, the values at Sites SLR 80 cm and SLR 40 cm increased by 7.4% and 13.5%. Furthermore, annual CO_2 emission was comparable between Sites SLR 40 cm and SLR 0 cm, which was approximately 4 times higher than that at Site SLR 80 cm (Table 3).

The CO_2-equivalent fluxes were estimated by the summation of three gas fluxes with values of 396.61 g/(m²·a), 1 423.29 g/(m²·a) and 1 420.21 g/(m²·a) at Sites SLR 80 cm, SLR 40 cm and SLR 0 cm, respectively. The minimum contributor to greenhouse effect was CH_4, only accounting for 1.06%–4.08% of CO_2-equivalent fluxes at the three sites. When it came to the greatest contributor to greenhouse effect, it was CO_2 for Sites SLR 0 cm, SLR 40 cm and SLR 80 cm, with a proportion reaching 83.91%–96.52% (Fig. 4).

Table 2. Pearson correlation coefficients (r) between soil-atmosphere greenhouse gas fluxes and soil properties

Greenhouse gas	OC	TN	TP	C/N
N_2O	0.133	0.168	0.232*	0.009
CH_4	0.171	0.299**	0.143	–0.163
CO_2	0.534**	0.537**	0.536**	0.121

Note: * and ** indicate significant r value at p<0.05 and p<0.01, respectively. OC: organic carbon; TN: total nitrogen; TP: total phosphorus; C/N: C/N content ratio.

Table 3. Estimation of annual emission of N_2O, CH_4 and CO_2 based on monthly greenhouse gas flux measurements from June 2013 to May 2014

Emission	SLR 80 cm	SLR 40 cm	SLR 0 cm
N_2O/(mg·m^{-2}·a^{-1})	159.83	108.98	218.65
CH_4/(mg·m^{-2}·a^{-1})	475.87	502.77	442.92
CO_2/(g·m^{-2}·a^{-1})	332.81	1 373.72	1 340.00

Note: SLR: sea level rise.

4 Discussion

Mangrove soils are known to constitute a net source of CO_2, CH_4 and N_2O (Chen et al., 2010, 2012, 2015, 2016). As shown in Table 4, in the previous studies, the fluxes of CO_2, CH_4 and N_2O ranged from 0.027 mmol/(m²·h) to 20.56 mmol/(m²·h) (Poungparn et al., 2009; Chen et al., 2010, 2015), from –130 μmol/(m²·h) to 5 168.6 μmol/(m²·h) (Chauhan et al., 2008; Chen et al., 2010, 2015), from 0.13 μmol/(m²·h) to 126 μmol/(m²·h) (Corredor et al., 1999; Chen et al., 2010, 2015, 2020a), respectively. In the present study, the fluxes of CO_2, CH_4 and N_2O at Site SLR 0 cm were 3.47 mmol/(m²·h), 3.13 μmol/(m²·h) and 0.57 μmol/(m²·h), respectively, which were in broad agreement with records from previous studies. However, the fluxes of CO_2, CH_4 and N_2O at Sites SLR 40 cm and SLR 80 cm were changed due to SLR. Compared with Site SLR 0 cm, N_2O decreased by approximately 27.3% at Site SLR 80 cm and 50.2% at Site SLR 40 cm. This flux is closely controlled by water level (tidal influence), soil oxygen availability, soil salinity and soil nutrient environments (Menyailo et al., 1997;

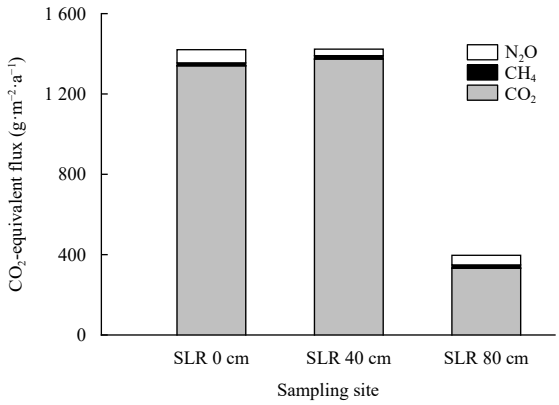

Fig. 4. CO_2-equivalent fluxes at the three *Kandelia obovata* forests. SLR: sea level rise.

Table 4. Soil-atmosphere fluxes of CO_2, CH_4 and N_2O from some mangrove forests

Location	CO_2 flux/(mmol·m^{-2}·h^{-1})	CH_4 flux/(μmol·m^{-2}·h^{-1})	N_2O flux/(μmol·m^{-2}·h^{-1})	Reference
Bay of La Parguera, Southwest Puerto Rico; Bird Island, Southwest Puerto Rico; Magueyes Island, Southwest Puerto Rico	ND	8.57–188.89	0.13–8.58	Corredor et al. (1999)
Bhitarkanika, eastern coast of India	ND	5.09–179.44	0.23–20.79	Chauhan et al. (2008)
The secondary mangrove forests of eastern Thailand	0.027–0.052	ND	ND	Poungparn et al. (2009)
Maipo Natural Reserve, Hong Kong, South China; Futian mangrove forest, Shenzhen, South China	0.69–20.56	11.9–5 168.6	0.14–23.83	Chen et al. (2010)
Jiulong River Estuary Mangrove Reserve	0.85–3.20	2.00–21.70	0.13–1.96	Chen et al. (2015)
Jiulong River Estuary Mangrove	ND	–130–1 800	4–126	Chen et al. (2020)

Note: ND: no determination of the *in situ* gas flux.

Inubushi et al., 1999; Chen et al., 2010; Jørgensen and Elberling, 2012). On the one hand, N_2O may be converted to N_2 or consumed before it gets emitted to the atmosphere depending upon the soil saturation status (Heincke and Kaupenjohann, 1999; Clough et al., 2005; Chapuis-Lardy et al., 2007; Chen et al., 2012). Higher soil water content found at Sites SLR 40 cm and SLR 80 cm resulted in soil in the saturation status (Chen et al., 2022b). N_2O may be converted to N_2 or consumed, resulting in lower N_2O fluxes at Sites SLR 80 cm and SLR 40 cm. On the other hand, salinity has been shown to inhibit complete denitrification (N_2O was converted to N_2 or consumed) due to the decrease in the proportion of N_2O reducing microorganisms with increasing salinization, potentially allowing for a build-up of N_2O (Menyailo et al., 1997; Inubushi et al., 1999). Low salinity levels at Sites SLR 80 cm and SLR 40 cm caused by SLR (Chen et al., 2022b) did not inhibit complete denitrification, resulting in less build-up of N_2O in the soils. Meanwhile, lower soil TN content, including inorganic nitrogen, which indirectly represented soil nutrient environments at Sites SLR 40 cm and SLR 80 cm, may limit microbes to generate N_2O which could explain the phenomenon in the present study.

Contrary to N_2O fluxes, CH_4 fluxes at Sites SLR 80 cm and SLR 40 cm were higher than that at Site SLR 0 cm. CH_4 fluxes are controlled by water levels and CH_4 fluxes will be discharged in large quantities at high water levels (Christensen et al., 2003; Wei et al., 2020). In the present study, higher soil water levels were found at Sites SLR 80 cm and SLR 40 cm compared with Site SLR 0 cm (Chen et al., 2022b). Water levels at Sites SLR 80 cm and SLR 40 cm may surpass the threshold which controlled CH_4 fluxes, resulting in higher CH_4 fluxes at Sites SLR 80 cm and SLR 40 cm. On the other hand, CH_4 fluxes in the mangrove environments were enhanced at the low salinity due to the intense oxidation or an alleviation of competition by the more energetically efficient sulfate- and nitrate-reducing bacteria than methanogenic archaea (Chen et al., 2010, 2018; Poffenbarger et al., 2011). Low soil salinity found at Sites SLR 80 cm and SLR 40 cm potentially decreased SO_4^{2-} availability which may be beneficial to methanogenic archaea, and stimulated CH_4 production, as reported in the other study (Stumm and Morgan, 1981). Finally, pH also affects methanogenic activity and the methanogenic archaea microbes are pH sensitive, and most of them grew over a relatively narrow pH range of about 6–8, with an optimum pH of 7.7 for activity of methane production methanogens in coastal wetlands (Chang and Yang, 2003). Soil pH increased with SLR (Chen et al., 2022b) and this parameter maybe another factor which stimulated CH_4 production at Sites SLR 40 cm and SLR 80 cm in the present study.

In the former studies, a negative relationship between water content and CO_2 fluxes was found (e.g., Alongi, 2009; Chen et al., 2010, 2012; Chambers et al., 2013). In the present study, mean inundation times at Sites SLR 80 cm, SLR 40 cm and SLR 0 cm were 10 h/d, 8 h/d and 6 h/d (i.e., 5 h, 4 h and 3 h per tide), respectively. Although higher soil water content was determined at Site SLR 40 cm, annual CO_2 fluxes at Sites SLR 40 cm and SLR 0 cm were similar. CO_2 fluxes decreased by approximately 75% only when the sea level rose to 80 cm. There may be a threshold of water levels that controls CO_2 fluxes and this threshold was opened at Site SLR 80 cm, resulting in low CO_2 fluxes at Site SLR 80 cm. Meanwhile, sulfate effect was a main biogeochemical driver that influenced OC cycling in the wetland soils (Chambers et al., 2013). The lowest soil salinity at Site SLR 80 cm decreased SO_4^{2-} availability and decrease of SO_4^{2-} availability inhibited sulfate reduction, which may result in a decrease of CO_2 fluxes. Furthermore, microbial biomass plays an important role in mangrove OC stocks, such as key role of root symbiotic microbiota in the decomposition of organic matter (Alongi, 2009). CO_2 emissions from soils raised from a variety of processes including autotrophic respiration, decomposition of organic matter via aerobic and anaerobic microorganisms (heterotrophic microbial respiration) (Poungparn et al., 2009; Capooci et al., 2019). Microbial biomass decreased due to anaerobic conditions and low nutrient environments, resulting in the low decomposition rate (Breithaupt et al., 2012). In the present study, soil TN contents which indirectly represented soil nutrient environments decreased with SLR and soil environments were under anaerobic conditions due to long periods of inundation, which would resulted in low CO_2 fluxes at Site SLR 80 cm. In addition, availability of OC is an important biogeochemical factor for soil CO_2 emissions. On the one hand, aboveground and belowground biomass, and leaf photosynthesis of *K. obovata* were suppressed at higher levels of flooding (Chen and Ye, 2013). Annual vegetation OC stock increments and vegetation OC stocks decreased with SLR (Chen et al., 2022a). These suggested that low vegetation biomass or OC stock may be contributing to the low soil CO_2 emissions at Site SLR 80 cm. On the other hand, soil CO_2 emissions were correlated with soil OC content and the lowest soil OC content (0–5 cm soil depth) was found at Site SLR 80 cm, resulting in low soil CO_2 emissions at Site SLR 80 cm.

In order to estimate the respective contributions of these three fluxes to CO_2-equivalent fluxes, all three greenhouse gas fluxes were converted to CO_2-equivalent fluxes on a 100 a time scale based on annual greenhouse gas fluxes. Mangrove soils at the three sites had a positive CO_2-equivalent fluxes, and CO_2-equivalent fluxes were comparable between Sites SLR 40 cm and SLR 0 cm due to CO_2 fluxes. However, the estimation of CO_2-equivalent fluxes from mangrove soils decreased under the influence of rising sea-level by 80 cm, which was attributed more to the decrease of N_2O and CO_2 fluxes at Site SLR 80 cm. On the other hand, CO_2 was the primary contributor of mangrove soils to CO_2-equivalent fluxes at Sites SLR 0 cm, SLR 40 cm and SLR 80 cm, as reported in the previous studies (Chen et al., 2010, 2012, 2015, 2016). However, SLR changed the contribution rates of CH_4 and N_2O fluxes to CO_2-equivalent fluxes. At Site SLR 80 cm, the contribution rate of CH_4 and N_2O to CO_2-equivalent fluxes were up to 4.08% and 12.01%. The warming potential of trace CH_4 and N_2O was non-negligible and should be considered in the evaluation of the warming effect on the soil gas emissions especially for mangrove forests and other coastal wetlands subjected to SLR.

Different intertidal elevations are used to represent different tidal flooding situations that might be expected with rising sea level. This study found the differences in the soil-atmosphere greenhouse gas emissions with SLR. However, some questions were not considered in this study. Firstly, three intertidal elevations were used to represent different tidal flooding situations of SLR and SLR impacts were not directly observed in this study. Some mangroves have adjusted to sea level rise and avoided submergence by accreting soil (Krauss et al., 2014). Adaptation of mangroves to SLR was not considered in the present study. Long-term observations of effect of SLR on the soil-atmosphere greenhouse gas emissions and even the whole mangrove ecosystem should be considered in the future studies. Secondly, sea levels were different at the different areas, and sea level may even reach 200 cm by the end of the 21st century based on Representative Concentration Pathway Scenarios (Mafi-Gholami et al., 2020).

Data of SLR was only based on the average increase in sea level in China. Considered with complexity of SLR, without a doubt, more samples should be collected at the different areas with different SLR conditions to fully clarify effects of SLR on the soil-atmosphere greenhouse gas emissions and even the whole mangrove ecosystem in the future studies. Finally, although potential effects and possible mechanisms of SLR on the soil-atmosphere greenhouse gas emissions were found through different tidal flooding situations of SLR, specific mechanisms of SLR on the three greenhouse gas emissions were not considered in the present study and specific mechanisms should be considered in the next studies.

5 Conclusions

In the present study, three intertidal elevations were used to represent different tidal flooding situations of SLR to clarify potential effects of SLR on the soil-atmosphere greenhouse gas emissions in mangrove soils. On the one hand, higher soil water content, and lower salinity and soil nutrition environments caused by SLR may limit microbes to generate N_2O which resulted in significantly lower N_2O fluxes at Site SLR 80 cm. Lower salinity, higher soil water content and soil pH caused by SLR stimulated CH_4 production at Sites SLR 80 cm and SLR 40 cm. Significantly lower CO_2 fluxes were found at Site SLR 80 cm due to higher soil water content, lower salinity, lower OC availability and soil nutrient environments. On the other hand, the lowest CO_2-equivalent fluxes were determined at Site SLR 80 cm due to lower N_2O and CO_2 fluxes. Contribution rates of N_2O and CH_4 to CO_2-equivalent fluxes were up to the highest value at Site SLR 80 cm and warming potential of trace CH_4 and N_2O was non-negligible with SLR. Therefore, potential effects of SLR on the soil-atmosphere greenhouse gas emissions and even blue carbon capability of the whole mangrove ecosystem should be attended continuously in the future studies.

Acknowledgements

The authors thank Yingying Huang, Jin Wang and Dan Liu for their helps in field sampling and laboratory chemical analysis. We thank the anonymous reviewers of this manuscript for their constructive comments.

References

Allen S E, Grimshaw H M, Parkinson J A, et al. 1974. Chemical Analysis of Ecological Materials. Oxford: Blackwell Scientific Publications

Alongi D M. 2009. The Energetics of Mangrove Forests. Dordrecht: Springer

Alongi D M. 2014. Carbon cycling and storage in mangrove forests. Annual Review of Marine Science, 6: 195–219, doi: 10.1146/annurev-marine-010213-135020

Breithaupt J L, Smoak J M, Smith III T J, et al. 2012. Organic carbon burial rates in mangrove sediments: strengthening the global budget. Global Biogeochemical Cycles, 26(3): GB3011

Capooci M, Barba J, Seyfferth A L, et al. 2019. Experimental influence of storm-surge salinity on soil greenhouse gas emissions from a tidal salt marsh. Science of the Total Environment, 686: 1164–1172, doi: 10.1016/j.scitotenv.2019.06.032

Chambers L G, Osborne T Z, Reddy K R. 2013. Effect of salinity-altering pulsing events on soil organic carbon loss along an intertidal wetland gradient: a laboratory experiment. Biogeochemistry, 115(1): 363–383

Chang Tsan-Chang, Yang Shang-Shyng. 2003. Methane emission from wetlands in Taiwan. Atmospheric Environment, 37(32): 4551–4558, doi: 10.1016/S1352-2310(03)00588-0

Chapuis-Lardy L, Wrage N, Metay A, et al. 2007. Soils, a sink for N_2O? A review. Global Biogeochemical Cycles, 13(1): 1–17

Chauhan R, Ramanathan A L, Adhya T K. 2008. Assessment of methane and nitrous oxide flux from mangroves along eastern coast of India. Geofluids, 8(4): 321–332, doi: 10.1111/j.1468-8123.2008.00227.x

Chen Guangcheng, Chen Jiahui, Ou Danyun, et al. 2020a. Increased nitrous oxide emissions from intertidal soil receiving wastewater from dredging shrimp pond sediments. Environmental Research Letters, 15(9): 094015, doi: 10.1088/1748-9326/ab93fb

Chen Yaping, Chen Guangcheng, Ye Yong. 2015. Coastal vegetation invasion increases greenhouse gas emission from wetland soils but also increases soil carbon accumulation. Science of the Total Environment, 526: 19–28, doi: 10.1016/j.scitotenv.2015.04.077

Chen Guangcheng, Chen Bin, Yu Dan, et al. 2016. Soil greenhouse gas emissions reduce the contribution of mangrove plants to the atmospheric cooling effect. Environmental Research Letters, 11(12): 124019, doi: 10.1088/1748-9326/11/12/124019

Chen Jiahui, Gao Min, Chen Guangcheng, et al. 2022a. Biomass accumulation and organic carbon stocks of *Kandelia obovata* mangrove vegetation under different simulated sea levels. Acta Oceanologica Sinica, 41(8): 78–86, doi: 10.1007/s13131-021-1891-2

Chen Guangcheng, Gao Min, Pang Bopeng, et al. 2018. Top-meter soil organic carbon stocks and sources in restored mangrove forests of different ages. Forest Ecology and Management, 422: 87–94, doi: 10.1016/j.foreco.2018.03.044

Chen Jiahui, Huang Yingying, Chen Guangcheng, et al. 2020b. Effects of simulated sea level rise on stocks and sources of soil organic carbon in *Kandelia obovata* mangrove forests. Forest Ecology and Management, 460: 117898, doi: 10.1016/j.foreco.2020.117898

Chen Guangcheng, Tam N F Y, Ye Yanlei. 2010. Summer fluxes of atmospheric greenhouse gases N_2O, CH_4 and CO_2 from mangrove soil in South China. Science of the Total Environment, 408(13): 2761–2767, doi: 10.1016/j.scitotenv.2010.03.007

Chen Guangcheng, Tam Nora F Y, Ye Yong. 2012. Spatial and seasonal variations of atmospheric N_2O and CO_2 fluxes from a subtropical mangrove swamp and their relationships with soil characteristics. Soil Biology and Biochemistry, 48: 175–181, doi: 10.1016/j.soilbio.2012.01.029

Chen Luzhen, Wang Wenqing. 2017. Ecophysiological responses of viviparous mangrove *Rhizophora stylosa* seedlings to simulated sea-level rise. Journal of Coastal Research, 33(6): 1333–1340

Chen Yaping, Ye Yong. 2013. Growth and physiological responses of saplings of two mangrove species to intertidal elevation. Marine Ecology Progress Series, 482: 107–118, doi: 10.3354/meps10274

Chen Yaping, Ye Yong. 2014. Early responses of *Avicennia marina* (Forsk.) Vierh. to intertidal elevation and light level. Aquatic Botany, 112: 33–40, doi: 10.1016/j.aquabot.2013.07.006

Chen Jiahui, Zhu Heng, Huang Yingying, et al. 2022b. Potential effects of sea level rise on decomposition and nutrient release of dead fine roots in a *Kandelia obovata* forest. Estuarine, Coastal and Shelf Science, 268: 107809

Christensen T R, Ekberg A, Ström L, et al. 2003. Factors controlling large scale variations in methane emissions from wetlands. Geophysical Research Letters, 30(7): 1414

Clough T J, Sherlock R R, Rolston D E. 2005. A review of the movement and fate of N_2O in the subsoil. Nutrient Cycling in Agroecosystems, 72(1): 3–11, doi: 10.1007/s10705-004-7349-z

Corredor J E, Morell J M, Bauza J. 1999. Atmospheric nitrous oxide fluxes from mangrove sediments. Marine Pollution Bulletin, 38(6): 473–478, doi: 10.1016/S0025-326X(98)00172-6

Davidson N C, Fluet-Chouinard E, Finlayson C M. 2018. Global extent and distribution of wetlands: trends and issues. Marine and Freshwater Research, 69(4): 620–627, doi: 10.1071/MF17019

Donato D C, Kauffman J B, Murdiyarso D, et al. 2011. Mangroves among the most carbon-rich forests in the tropics. Nature

Geoscience, 4(5): 293–297, doi: 10.1038/ngeo1123
Heincke M, Kaupenjohann M. 1999. Effects of soil solution on the dynamics of N_2O emissions: a review. Nutrient Cycling in Agroecosystems, 55(2): 133–157, doi: 10.1023/A:1009842011599
Inubushi K, Barahona M A, Yamakawa K. 1999. Effects of salts and moisture content on N_2O emission and nitrogen dynamics in yellow soil and andosol in model experiments. Biology and Fertility of Soils, 29(4): 401–407, doi: 10.1007/s003740050571
IPCC. 2013. Climate Change: The Physical Science Basis. Contribution of Working Group I to the Fifth Assessment Report of the Intergovernmental Panel on Climate Change. Cambridge: Cambridge University Press
Jayanthi M, Thirumurthy S, Samynathan M, et al. 2018. Shoreline change and potential sea level rise impacts in a climate hazardous location in southeast coast of India. Environmental Monitoring and Assessment, 190(1): 51, doi: 10.1007/s10661-017-6426-0
Jørgensen C J, Elberling B. 2012. Effects of flooding-induced N_2O production, consumption and emission dynamics on the annual N_2O emission budget in wetland soil. Soil Biology and Biochemistry, 53: 9–17, doi: 10.1016/j.soilbio.2012.05.005
Kirwan M L, Gedan K B. 2019. Sea-level driven land conversion and the formation of ghost forests. Nature Climate Change, 9(6): 450–457, doi: 10.1038/s41558-019-0488-7
Krauss K W, McKee K L, Lovelock C E, et al. 2014. How mangrove forests adjust to rising sea level. New Phytologist, 202(1): 19–34, doi: 10.1111/nph.12605
Langston A K, Kaplan D A, Putz F E. 2017. A casualty of climate change? Loss of freshwater forest islands on Florida's Gulf Coast. Global Change Biology, 23(12): 5383–5397, doi: 10.1111/gcb.13805
Liikanen A, Martikainen P J. 2003. Effect of ammonium and oxygen on methane and nitrous oxide fluxes across sediment-water interface in a eutrophic lake. Chemosphere, 52(8): 1287–1293, doi: 10.1016/S0045-6535(03)00224-8
Liu Chuan, Li Ya, Wang Hui. 2019. Ocean Blue Book on Climate Change in China in 2019 (in Chinese). Tianjin: National Oceanographic Information Center, Ministry of Natural Resources of the People's Republic of China
Lovelock C E, Cahoon D R, Friess D A, et al. 2015. The vulnerability of Indo-Pacific mangrove forests to sea-level rise. Nature, 526(7574): 559–563, doi: 10.1038/nature15538
Mafi-Gholami D, Zenner E K, Jaafari A. 2020. Mangrove regional feedback to sea level rise and drought intensity at the end of the 21st century. Ecological Indicators, 110: 105972, doi: 10.1016/j.ecolind.2019.105972
McLeod E, Chmura G L, Bouillon S, et al. 2011. A blueprint for blue carbon: toward an improved understanding of the role of vegetated coastal habitats in sequestering CO_2. Frontiers in Ecology and the Environment, 9(10): 552–560, doi: 10.1890/110004
Meeder J F, Parkinson R W, Ogurcak D, et al. 2021. Changes in sediment organic carbon accumulation under conditions of historical sea-level rise, Southeast Saline Everglades, Florida, USA. Wetlands, 41(4): 41, doi: 10.1007/s13157-021-01440-7
Menyailo O V, Stepanov A L, Umarov M M. 1997. The transformation of nitrous oxide by denitrifying bacteria in Solonchaks. Eurasian Soil Science, 30(2): 178–180
Minick K J, Mitra B, Noormets A, et al. 2019. Saltwater reduces potential CO_2 and CH_4 production in peat soils from a coastal freshwater forested wetland. Biogeosciences, 16(23): 4671–4686, doi: 10.5194/bg-16-4671-2019
Myhre G, Shindell D, Bréon F M, et al. 2013. Anthropogenic and natural radiative forcing. In: Stocker T F, Qin D, Plattner G K, et al., eds. Climate Change 2013: The Physical Science Basis. Contribution of Working Group I to the Fifth Assessment Report of the Intergovernmental Panel on Climate Change. Cambridge: Cambridge University Press
Perera K A R S, De Silva K H W L, Amarasinghe M D. 2018. Potential impact of predicted sea level rise on carbon sink function of mangrove ecosystems with special reference to Negombo estuary, Sri Lanka. Global and Planetary Change, 161: 162–171, doi: 10.1016/j.gloplacha.2017.12.016
Poffenbarger H J, Needelman B A, Megonigal J P. 2011. Salinity influence on methane emissions from tidal marshes. Wetlands, 31(5): 831–842, doi: 10.1007/s13157-011-0197-0
Poungparn S, Komiyama A, Tanaka A, et al. 2009. Carbon dioxide emission through soil respiration in a secondary mangrove forest of eastern Thailand. Journal of Tropical Ecology, 25(4): 393–400, doi: 10.1017/S0266467409006154
Rogers K, Kelleway J J, Saintilan N, et al. 2019. Wetland carbon storage controlled by millennial-scale variation in relative sea-level rise. Nature, 567(7746): 91–95, doi: 10.1038/s41586-019-0951-7
Ruan Hailin, Yang Yanming, Li Yanchu, et al. 2010. Study of the variation in sea level around Taiwan Island during the last 16 years. Journal of Oceanography in Taiwan Strait (in Chinese), 29(3): 394–401
Sheng Nong, Wu Feng, Liao Baowen, et al. 2021. Methane and carbon dioxide emissions from cultivated and native mangrove species in Dongzhai Harbor, Hainan. Ecological Engineering, 168: 106285, doi: 10.1016/j.ecoleng.2021.106285
Stumm W, Morgan J J. 1981. Aquatic Chemistry: An Introduction Emphasizing Chemical Equilibria in Natural Waters. 2nd ed. New York: John Wiley & Sons, 448–463
Wang Gang, Guan Dongsheng, Xiao Ling, et al. 2019. Ecosystem carbon storage affected by intertidal locations and climatic factors in three estuarine mangrove forests of South China. Regional Environmental Change, 19(6): 1701–1712, doi: 10.1007/s10113-019-01515-6
Wei Siyu, Han Guangxuan, Chu Xiaojing, et al. 2020. Effect of tidal flooding on ecosystem CO_2 and CH_4 fluxes in a salt marsh in the Yellow River Delta. Estuarine, Coastal and Shelf Science, 232: 106512
Ye Yong, Gu Yantao, Gao Haiyan, et al. 2010. Combined effects of simulated tidal sea-level rise and salinity on seedlings of a mangrove species, *Kandelia candel* (L.) Druce. Hydrobiologia, 641(1): 287–300, doi: 10.1007/s10750-010-0099-9
Zhang Zhen, Fluet-Chouinard E, Jensen K, et al. 2021. Development of the global dataset of Wetland Area and Dynamics for Methane Modeling (WAD2M). Earth System Science Data, 13(5): 2001–2023, doi: 10.5194/essd-13-2001-2021